PROCEEDINGS OF SCIENCE

Spectroscopic study of heavier quark baryons using hadron beam at J-PARC

Kotaro Shirotori[a,*]

[a] *Research Center for Nuclear Physics (RCNP), Osaka University, 10-1 Mihogaoka, Ibaraki, Osaka, Japan*

E-mail: sirotori@rcnp.osaka-u.ac.jp

Understanding hadron formation is one of the fundamental goals of hadron physics. Spectroscopic observations of charmed and multi-strange baryons can provide a unique opportunity to study internal structure of hadrons. Systematic studies of charmed and multi-strange baryons are expected to reveal effective degrees of freedom and their interaction for describing hadron structures. The hadron experimental facility at J-PARC aims at revealing hadron structures using the world's most intense meson beam. The high-intensity and high-momentum beams can provide many opportunities to investigate the structure of hadrons, in which charm and strange quarks play an important role. High-momentum beam line, called the π20 beam line, is under construction, and the charmed baryon spectroscopy experiment is planned. In the future, the Hadron Experimental Facility are extended to include beam lines with special capabilities. Dedicated high-momentum beam line called the K10 beam line, which can provide separated K^- up to 10 GeV/c, is planned to be constructed. We promote systematic studies of charmed and multi-strange baryons using intense hadron beams at J-PARC.

The XVIth Quark Confinement and the Hadron Spectrum Conference (QCHSC24)
19-24 August, 2024
Cairns Convention Centre, Cairns, Queensland, Australia

*Speaker

 ISSN 1824-8039 . Published by SISSA Medialab.

PoS(QCHSC24)133

1. Introduction

Hadrons consists of quarks and gluons interacting with each other. The goal of hadron physics is to answer the question "how quarks build hadrons". The resulting knowledge for explaining various properties of observed hadrons and predicting new phenomena can be used as a basis for various extended studies where hadrons appear, such as dense hadronic matter. Furthermore, QCD is the only gauge theory that shows a non-perturbative nature of the dynamics and can be accessed experimentally. Thus, the study of QCD should help to understand what happens in various other physical systems. The spectroscopy of hadrons has been studied for many years, mostly driven by the experimental discovery of new states [1]. Recently, lattice QCD has made crucial contributions to establishing that QCD is indeed the theory of the strong interaction for hadrons, and has even opened a path from QCD to nuclear systems. Nevertheless, there are still open or unresolved questions. They are important not only for their own sake, but also because of their broad application to related fields. For example, the question of high-density hadronic matter is considered to be one of the most challenging problems in the physics of the strong interaction, QCD.

Based on the general descriptions above, there are several important aspects in hadron physics. First, different favour combinations of quarks with different masses would lead to non-trivial flavor-dependent dynamics, although the fundamental interaction of quarks and gluons is flavor blind. The quarks are classified into light u, d, s quarks and heavy c, b quarks by comparing their masses with the QCD scale parameter Λ_{QCD}. The position of the s quark is somewhat subtle, as it is neither as light as the u, d quarks nor as heavy as the c quarks, leading to interesting observations in hadrons containing strange quarks. Second, there are large spin-dependent forces. This is in contrast to atomic systems, for example, which are governed by electromagnetic interactions. Sufficiently attractive spin-spin forces lead to strong correlation in quark pairs, diquark, in their antisymmetric spin and flavour channels in the orbital ground state, which plays a crucial role not only in spectroscopy but also in high-density hadronic matter where the colour superconducting phase is expected to form. For spectroscopy, we also consider the internal structure of the diquark with orbital excitation. Different flavor combinations, in particular those of u, d, s quarks, can lead to different properties. Strongly correlated diquark are also thought to be important for exotic hadrons with multiquark contents. Therefore, a detailed knowledge of the spin dependent interaction for u, d, s quarks is a very important issue that can be studied at π20 and K10 beam lines in the J-PARC hadron experimental facility.

1.1 Charmed baryon spectroscopy

Since the charm (c) quark is much heavier than the u and d quarks, the internal motions of the ud quarks can be distinguished from those of the c quark in charmed baryons. It can be seen that the orbital excitation energy of an ud pair to c (λ mode) is lower than that between u and d (ρ mode), as shown in Fig. 1(a). This is a kinematic effect under the confinement potential known as the isotope shift. In addition, the spin-spin interaction with the c quark is suppressed, since the colour-magnetic interaction between two quarks is proportional to the inverse of the respective quark mass. The spin singlet state ud is of particular interest, since its interaction is attractive. This is where the ud diquark correlation comes from. Therefore, baryons with a c quark provide a good

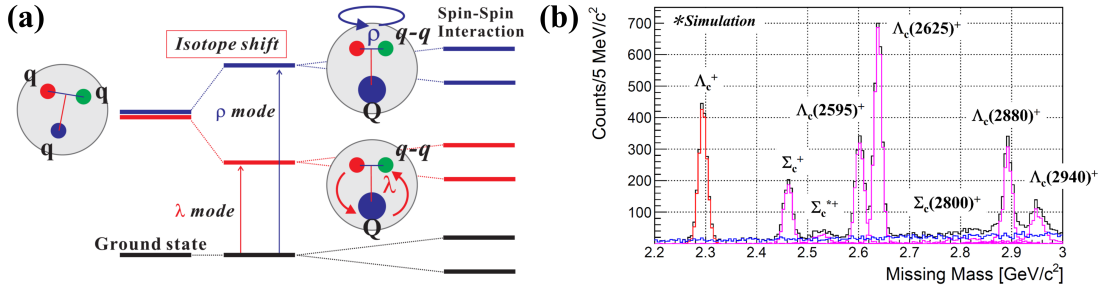

Figure 1: (a) Schemtic illustration of the isotop shift effect in excited charmed baryons. The excition energy of the λ-mode state is lower than that of the ρ-mode state. (b) Simulated missing mass spectrum of charmed baryons at the incident pion momentum of 20 GeV/c. The spectrum is obtained by the missing mass of the $\pi^- p \to D^{*-} Y_c^{*+}$ reaction for the generated Y_c^*-produced events and background processes. The contribution from the ground-state Λ_c^+ is plotted in red, and that from each excited state (Λ_c^* or Σ_c^*) is represented in magenta. The background contribution is shown in the blue histogram.

opportunity to study the ud diquark correlation. We also expect to decipher the origin of the quark interactions by analyzing the high-statistics data in terms of QCD-based effective theories.

We have proposed charmed baryon spectroscopy experiment approved as E50 [2] at the J-PARC high-momentum beam line (π20). To produce charmed baryons, missing-mass technique is employed via the $\pi^- p \to D^{*-} Y_c^{*+}$ reaction, where Y_c^{*+} represent excited charmed baryons. A series of the Y_c^{*+} states will be observed in the missing mass spectrum as shown in Fig. 1(b). The production rates of the excited states are expected to depend on their internal configurations of spins and orbital angular momenta (parity). In the $\pi^- p \to D^{*-} Y_c^{*+}$ reaction, a u quark in the proton is converted into a c quark in the charmed baryon Y_c^{*+}, which we call the one-quark process, is expected to dominate [3]. In the one-quark process, the angular momentum is introduced between c and ud. Thus, the λ mode excited states are favoured to be populated in the one quark process. The reaction cross section is estimated by calculating the so-called sticking probability of c to ud, written as

$$\left|\langle \varphi_f(\boldsymbol{r}) | 2\sigma_- \exp(-i\boldsymbol{q}\boldsymbol{r}) | \varphi_i(\boldsymbol{r}) \rangle\right|^2 \propto (q/\alpha)^{2L} \exp(-q^2/\alpha^2),$$

where $\varphi_{i(f)}$, L, q, and α represent an initial u (a final c) wave function, the angular momentum introduced in the charmed baryons, the momentum transfer of the reaction, and a typical size parameter of baryon (~0.4 GeV/c), respectively. Here, σ_- is a spin operator required in the case of a vector meson exchange in the reaction. In the right-hand side of the above equation, the wave functions of the initial and final states for the harmonic oscillator potential are used for the analytical calculations. Since the reaction involves a large momentum transfer of q ~1.4 GeV/c, the cross section including the sticking probability becomes very small due to the exponential factor. The intense pion beam provided by the π20 beam line compensates for the small cross sections. On the other hand, if we consider the ratio of the cross section of the excited state with L to that of the ground state, the exponential factor is almost cancelled out, and the ratio does not decrease due to the factor of $(q/\alpha)^{2L}$. The relatively high possibility to populate the higher excited states with a finite L is rather advantageous.

1.2 Ω baryon spectroscopy

The Ω baryon is a system of three strange quarks, sss. In the SU(3) flavor symmetry group, it is assigned as a member of the decuplet representation realized by the quark model whose building blocks are the u, d and s quarks. In reality, the SU(3) symmetry is broken by the mass of the s quark, which is heavier than the nearly equal masses of the u, d quarks. The pattern of SU(3) breaking could predict the mass of Ω under equal mass spacing between the decuplet members. The broken SU(3) also leads to the apparent mass difference between the pion ($m_\pi \sim 140$ MeV) and the kaon ($m_K \sim 500$ MeV). This difference, together with the single flavour nature, leads to the unique properties of the Ω baryons. The Ω baryons do not couple to the pion due to isospin symmetry. Therefore, without the meson cloud present in the light baryon structure, we may be able to directly access the quark core region of the baryons. Furthermore, we can expect that an Ω baryon will be smaller in size compared to the light flavoured baryons which are surrounded by a meson cloud.

The current state of Ω baryon spectroscopy is poor, so it has not yet reached the stage where data can be compared with theory. Nevertheless, we would like to discuss Ω spectroscopy in some detail. First, the sss combination imposes some restrictions on the wave function due to Pauli's exclusion principle. For example, the fact that the spin of the ground state Ω is 3/2 instead of 1/2 is due to this requirement. Similar constraints apply to excited states. Some consequences of the restrictions can be seen in the fine structures of the excited states. We propose the experiment to study Ω baryons at the J-PARC hadron experimental facility [4].

2. High-momentum secondary beam lines at J-PARC

2.1 π20 beam line

Since the beginning of 2020, the high-p beam line (High-p) has been operated with a primary beam branched from the existing slow-extraction beam line(A line). High-p is designed to transport the secondary beam produced with a 15-kW loss target at the branching point in the A line(Fig. 2). The beam line is called "π20". The secondary beam with a negative charge produced at zero degrees at the production target is departed from the primary beam course (A line) to the π20 beam line by using the so-called beam swinger optics [5]. The layout is optimized to deliver the negative-charge secondary beam with a momentum of 20 GeV/c produced at zero degrees extracted to the π20 beam line. The expected beam intensity at 20 GeV/c is several 10 M/spill(2.0 second extraction time). Secondary beam is collected by the first doublet of quadrupole magnets in the π20 beam line and focused at a collimator placed 50 m downstream from the production target to define the beam image at the production target. After the collimator, the beam is focused again at the dispersive focal plane with a large dispersion. Beam line magnets are employed to eliminate/minimize major geometric and chromatic aberrations to the second order. The correlation of the horizontal position (x) to the momentum (dispersion dp/p) of beam particles at the dispersive focal plane gives momentum of the secondary beam. A momentum resolution as good as 0.1%(σ) can be realized with a spatial resolution of 1 mm for a beam particle. The horizontal and vertical beam profiles and the angle of incidence relative to the beam direction at the experimental target as estimated around 20 mm and 10 mrad for position and angular distributions, respectively.

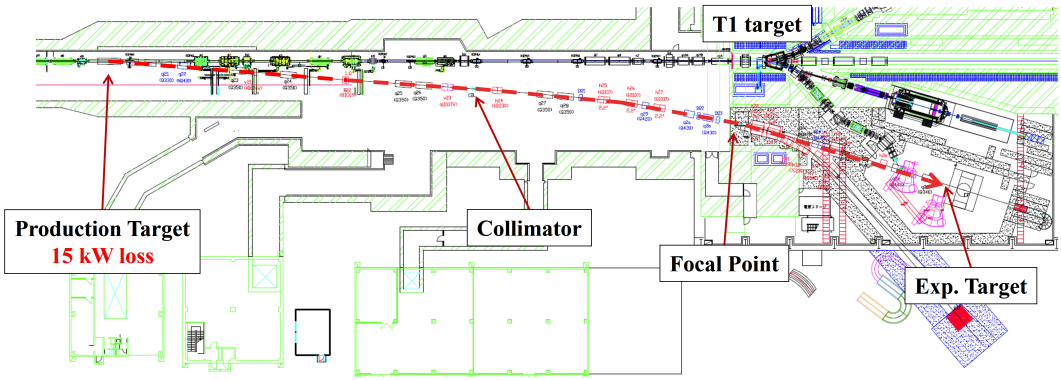

Figure 2: Floor plan of the southern part in the hadron hall and the π20 beam line.

2.2 K10 beam line

A high-intensity, high-momentum and high-purity K^- beam is an essential component of the Ω baryon spectroscopy experiment. Therefore, the K10 beam line under discussion in the "Hadron Experimental Facility Extension" project [6] is the unique place where the Ω baryon spectroscopy experiment can be performed. The K10 beam line is designed for high momentum separated secondary beams such as K^- and anti-proton. The beam line consists of three sections: the front-end section, the separation section and the analysis section. In the front-end section, the secondary beams produced at the production target are extracted from the primary beam line and vertically focused at the intermediate slit to reduce the "background pions". The optics are also tuned to make the beams nearly achromatic at the IF slit. In the separation section we use a radio frequency (RF) separator to select the particles. After analysis with a beam spectrometer, the beam is focused in both horizontal and vertical directions onto an experimental target. The expected K^- beam intensity and momentum resolution are several M/spill and 0.1%(σ), respectively. In addition, due to the RF separator, the ratio of K^- to π^- in the beam delivered by the K10 beam line is 1:2, allowing the delivery of a high purity K^- beam.

3. MARQ Spectrometer

Figure 3 shows the schematic view of the MARQ spectrometer. MARQ means a Multipurpose Analyzer for Resonance and Quark dynamics in hadrons and hadronic systems. The MARQ spectrometer satisfies requirements of all the planned spectroscopy experiments at π20 and K10. In the E50 experiment, the charmed baryons (Y_c^{*+}'s: a generic term of Λ_c^*'s and Σ_c^*'s) are produced in the $\pi^- p \to Y_c^{*+} D^{*-}$ reaction. The Y_c^{*+} mass is determined from the $p(\pi^-, D^{*-})$ missing mass by detecting the final-sate $K^+\pi^-\pi^-$ particles from the D^{*-} decay. The daughter particles from the Y_c^{*+} decay are also planned to be detected. The E50 spectrometer is designed for detecting all the charged particles produced in the $\pi^- p \to Y_c^{*+} D^{*-}$ reaction at an incident pion momentum of 20 GeV/c. Emitted at forward angles are high-momentum particles from the $D^{*-} \to \bar{D}^0\pi^-$ decay followed by $\bar{D}^0 \to K^+\pi^-$ as well as daughter particles from the Y_c^{*+} decay. The momenta of the emitted particles range from 0.2 to 16 GeV/c. The stationary target is placed just in front of the entrance of the dipole magnet.

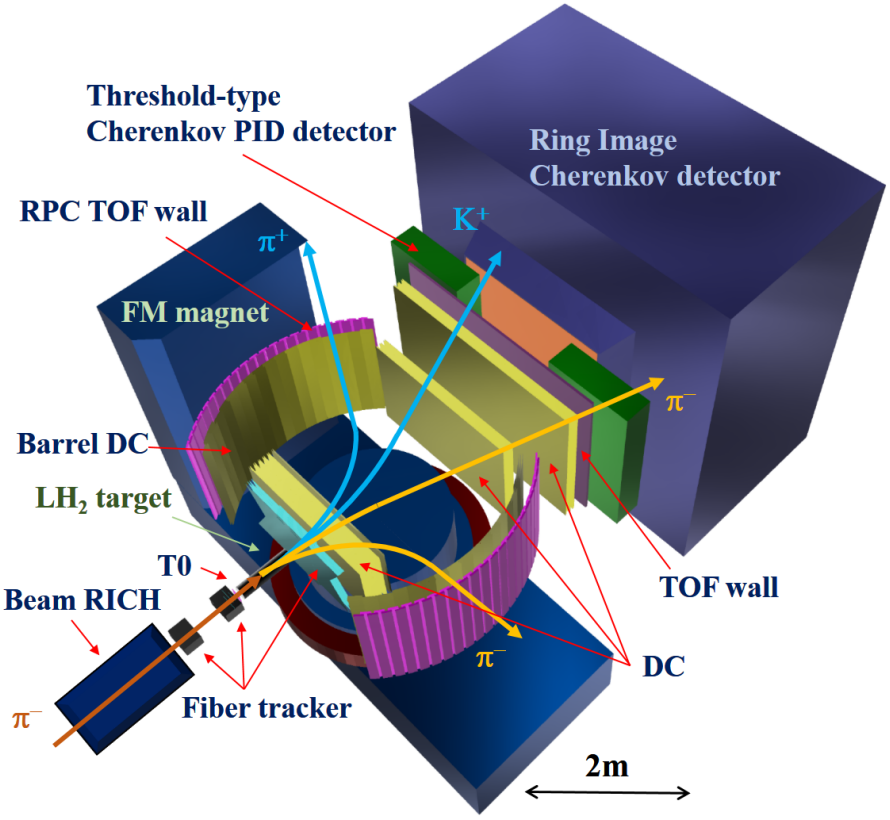

Figure 3: Schematic view of the MARQ spectrometer to be constructed for the E50 experiment at J-PARC. It consists of a large dipole magnet, tracking detectors, time-of-flight detectors, and particle-identification detectors. Some of tracking detectors and time-of-flight detectors are placed inside the gap of the magnet (internal detectors). The MARQ spectrometer is a general purpose spectrometer system to be used for various hadron spectroscopy experiments.

The MARQ spectrometer consists of a large dipole magnet, tracking detectors, time-of-flight detectors, and particle-identification detectors. To determine the Y_c^{*+} mass from the $p(\pi^-, D^{*-})$ missing mass, it is necessary to measure the four-momenta of the final-sate $K^+\pi^-\pi^-$ particles. Since high-momentum K^+ and π^- from the $\bar{D}^0$ decay are emitted at forward angles, placed at forward angles are scintillating-fiber hodoscopes [7] behind the target, several drift chambers (DCs), and ring-imaging Cherenkov detector (RICH) for the trajectory determination (momentum analysis), time-of-flight (TOF) measurement, and particle identification, respectively. Additional tracking and time-of-flight detectors are placed inside the gap of the magnet (internal detectors) to detect the slow π^-s emitted at forward angles from the D^{*-} decay (not from the $\bar{D}^0$ decay) and daughter particles from the Y_c^{*+} decay. These detectors should have a wide angular coverage since the slow π^-s cannot reach the exit of the dipole magnet and since the daughter particles are emitted in a wide angle range. The barrel-shaped DCs and high time-resolution TOF detector wall consisting of resistive-plate chambers (PRCs) are placed inside the gap of the magnet for detecting the slow π^- and horizontally-emitted Y_c^{*+} daughter particles. The RPCs are also placed on the pole pieces for detecting vertically-emitted Y_c^{*+}. The scintillating-fiber hodoscopes and DCs located behind the target are used not only for high-momentum $K^+\pi^-$ particles at forward angles but also for

all the produced particles. To get high-counting-rate capability, the scintillating-fiber hodoscopes are planned to be used just behind the target. They are also placed at upstream of the target for measuring the incident momentum and profile, or (x, y) intensity map. To get the reference timing for all the detectors, a fine-segmented acrylic Cherenkov counter (time-zero counter) [8] is placed just in front of the target. Another RICH counter, Beam RICH [9], is used for identifying incident particles in the secondary beam located at most upstream.

Since an expected cross section of charmed baryon at 20 GeV/c is as small as 1–10 nb, we will irradiate an intense pion beam of 30 Mcps in a 2.0 seconds extraction time on the liquid hydrogen target of 4 g thickness. The reaction rate is expected to be a few million per second, which is estimated from the total cross section of ~25 mb of the $\pi^- p$ reaction at 20 GeV/c. Then, the estimated data rate will be 13 GB per second (100 Gbps). To handle the large data flow, we adopted a streaming-readout data acquisition (SRODAQ) system [10]. SRODAQ is based on a parallel processing framework to handle data that is continuously sent from front-end electronics with a time stamp. All the detector signals are digitized in front-end electronics, and the digitized data fragments are continuously transfered (streaming) to a personal computers (PCs). The events of interest are selected using software on PCs by combining the streaming data fragments. In a streaming DAQ system, a complicated hardware trigger system is not necessary, which makes a busy time for processing an event corresponding to a trigger. We are developing a streaming DAQ system primarily for the MARQ spectrometer as well as special time-to-digital converters (TDCs) for a continuous time measurement without any external trigger. We have tested and successfully demonstrated the SRODAQ system using actual hadron beam at the J-PACR hadron experimental facilty [11]. The streaming DAQ system allows us to make the DAQ efficiency close to 100% without any trigger bias.

4. Baryon spectroscopy experiments

At the π20 and K10 beam lines, we conduct spectroscopy of Λ_c and Σ_c baryons (charmed baryons) as well as that of Ω baryon. At π20, excited Λ_c (Σ_c) baryons, Λ_c^*'s (Σ_c^*'s), are produced in the two-body $\pi^- p \to D^{*-}\Lambda_c^{*+}$ ($\pi^- p \to D^{*-}\Sigma_c^{*+}$) reaction, and they are identified from the $p\,(\pi^-, D^{*-})$ missing mass. Similarly, excited Ω baryons, Ω^*'s, are produced in $K^- p \to \Omega^{*-} K^+ K^{*0}$, and they are identified from the $p(K^-, K^+ K^{*0})$ missing mass.

4.1 Expected mass spectrum of charmed baryon spectroscopy

We investigate primarily the masses and decays of excited charmed baryons (Y_c^{*+}'s) in the $\pi^- p \to D^{*-} Y_c^{*+}$ reaction at an incident pion momentum of 20 GeV/c. The decay chain of the D^{*-} meson, $D^{*-} \to \bar{D}^0 \pi^-$ (branching ratio: 67.7%) and $\bar{D}^0 \to K^+ \pi^-$ (branching ratio: 3.95%), is used for determining the mass of the produced Y_c^*'s. Fig. 4 shows the expected Y_c^*-mass spectrum including the background contribution at the π20 beam line. The cross section of the ground state(Λ_c^+) of 1 nb at the incident pion momentum of 20 GeV/c is assumed to obtain this mass spectrum with a 100-day beam time. The production rate of Y_c^{*+}'s in $\pi^- p \to D^{*-} Y_c^{*+}$ were originally estimated using a Regge model where vector-meson (D^*) exchange dominates (one-quark process) [12]. In this estimation, a λ-mode excitation is likely to take place, and Σ_c^*'s are hardly observed. The relative production rates of $\Lambda_c(2286)1/2^+$, $\Sigma_c(2455)1/2^+$, and $\Sigma_c(2520)3/2^+$

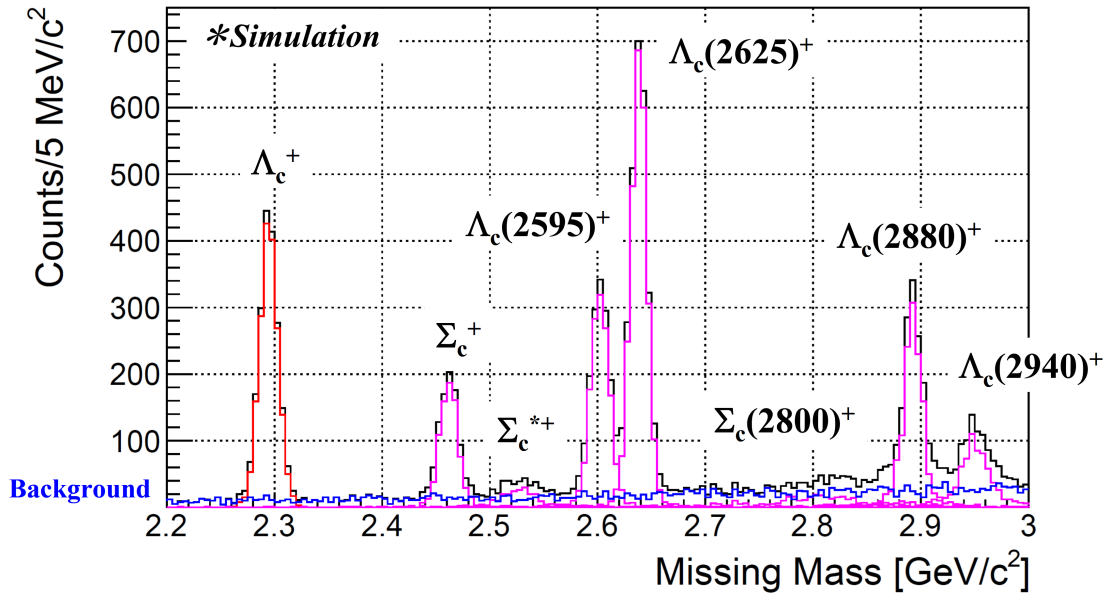

Figure 4: Expected Y_c^*-mass spectrum including the background contribution at the incident pion momentum of 20 GeV/c in a 100-day beam time. The spectrum is obtained by the $p(\pi^-, D^{*-})$ missing mass for the generated Y_c^*-produced events and background processes. The background contribution shown in the blue histogram is estimated by JAM [14]. It should be noted that the background contribution is highly suppressed owing to D^{*-} tagging. The contribution from the ground-state Λ_c^+ is plotted in red, and that from each excited state (Λ_c^* or Σ_c^*) is represented in magenta.

are 1.00, 0.03, and 0.17, respectively. A new reaction mechanism was proposed which considers the diquark correlation in baryons (two-quark process) [3]. This new mechanism causes both the λ- and ρ-mode excitations, In this case, the relative production rates become 1.0, 2.9, and 0 for $\Lambda_c(2286)1/2^+$, $\Sigma_c(2455)1/2^+$, and $\Sigma_c(2520)3/2^+$, respectively. Since both the mechanisms give the extreme relative ratio of $\Sigma_c(2455)1/2^+$ to the ground-state $\Lambda_c(2285)1/2^+$, we consider both the one- and two-quark processes are mixed in the real situation. Here, the mixing ratio is determined so that the production rate of the ground-state Λ is twice as much as that of the ground-state Σ to reproduce the experimental data in the strangeness sector [13]. In Fig. 4, the yield for each Y_c^* state is obtained using the corresponding relative production rate. The production cross section for $\Lambda_c(2286)1/2^+$ is fixed at 1 nb. The number of events expected for the ground-state $\Lambda_c(2285)1/2^+$ production is ~2000 in a 100-day beam time. It should be noted that the mass resolution is $\sim$ 8 MeV (σ) for Y_c^*'s. The background contribution is estimated by using the JAM code [14]. We expect to observe not only $\Lambda_c^{(*)}$'s but also $\Sigma_c^{(*)}$'s. The two heavy-quark spin doublets would appear corresponding to the P- and D-wave λ-mode excitations, $\Lambda_c(2595)1/2^-$-$\Lambda_c(2625)3/2^-$ and $\Lambda_c(2880)5/2^+$-$\Lambda_c(2940)3/2^+$, respectively. We can assign the excitation mode (λ or ρ) for Y_c^* from the production measurement.

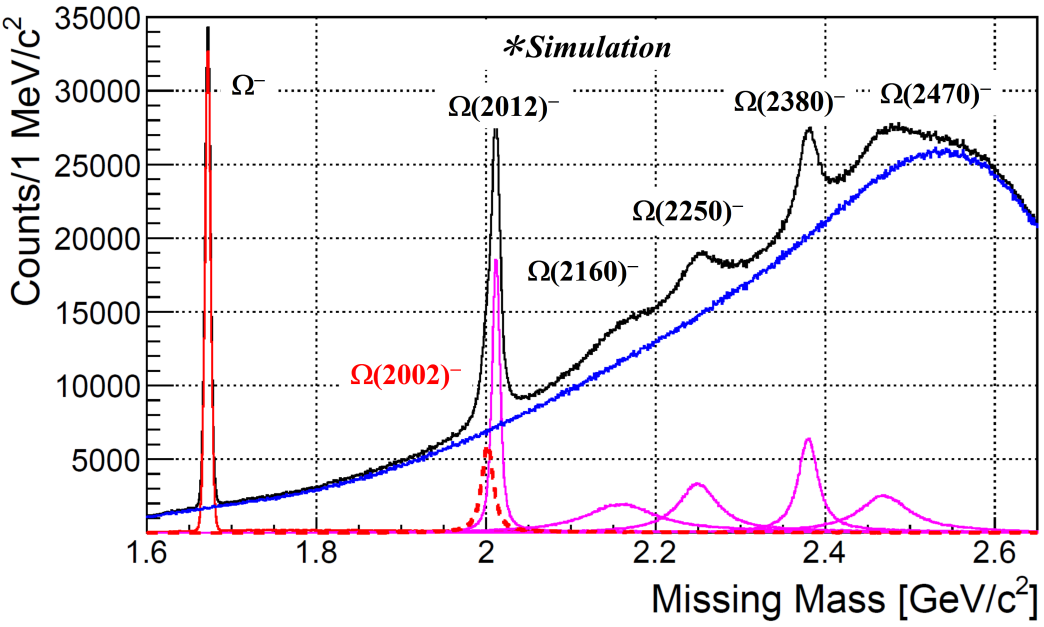

Figure 5: Expected $\Omega^{(*)-}$-mass spectrum including background contributions at the incident kaon momentum of 8 GeV/c in a 100-day beam time. The spectrum is obtained by the $p(K^-, K^+K^{*0})$ missing mass for the generated $\Omega^{(*)-}$-produced events and background processes. The smooth blue curve represent the background contribution estimated by JAM, and the contributions from the ground-state Ω^- and Ω^{*-}'s are also plotted in red and in magenta, respectively. The $p(K^-, K^+K^{*0})$ missing system gives $S = -3$, which eliminates huge background from Σ^*-produced events.

4.2 Expected mass spectrum of Ω baryon spectroscopy

We plan to investigate the masses and decays of excited Ω baryons (Ω^*s) in the $K^-p \to \Omega^{*-}K^+K^{*0}$ reactions at incident kaon momenta ranging from 7 to 10 GeV/c. Spectroscopy of Ω^*'s is a unique testing ground to reveal diquark correlation by comparing other sectors since neither diquark correlation nor pion cloud is expected in an Ω^* system. The mass of a produced Ω^* including the ground-state Ω ($\Omega^{(*)}$) can be determined in a missing-mass technique using the four-momenta of the initial-state K^-p and final-state $K^+K^+\pi^-$ in the $K^-p \to \Omega^{(*)-}K^+K^{*0}$ reaction. Here, the selected events are those in which the $K^+\pi^-$ invariant mass should give the K^{*0} mass.

Figure 5 shows the expected $\Omega^{(*)}$-mass spectrum including the background contribution at an incident kaon momentum of 8 GeV/c at the K10 beam line. The background contribution is estimated by using the JAM code [14]. The $\Omega^{(*)-}$ mass is calculated by the $p(K^-, K^+K^{*0})$ missing mass, and the cross section of $K^-p \to \Omega^{(*)-}K^+K^{0*}$ for each $\Omega^{(*)-}$ is assumed to be 63 nb. The number of events for each peak is $\sim 3.3\times10^5$, which can be obtained in a 100-day beam time. Since the number of events is large, the precision of the mass determination in this spectrum is better than 1 MeV depending on the width of the corresponding $\Omega^{(*)-}$. To get accuracy of the mass determination, the absolute momentum scale in the spectrometer is required to be calibrated carefully. We can

use various peaks corresponding to hyperons and other baryons in similar mass spectra. Thus, the accuracy would be also better than 1 MeV after the calibration. It is difficult to accurately determine the width of an $\Omega^{(*)-}$. The observed peak must be modified by the experimental mass resolution of 2.5–4.5 MeV (σ). The peak may be different in shape from the Breit-Wigner function owing to the overlap with other peaks and background processes including the interference effects. The accuracy of the width determination expected is better than 1 MeV for an isolated Breit-Wigner peak with a width of 10 MeV. We expect the accuracy of the width determination is better than a few MeV for high-mass Ω^*s, which are overlapped with other contributions.

In Fig. 5, $\Omega(2002)^-$ is also shown as the *LS* partner of $\Omega(2012)^-$ with a mass of 2.002 GeV and a width of 12 MeV (twice the $\Omega(2012)^-$ width). The production cross section of $\Omega(2002)^-$ is assumed to be a half that of $\Omega(2012)^-$. Although we cannot clearly observe the peak of $\Omega(2002)^-$ in the expected mass spectrum, the $\Omega(2002)^-$ contribution appears in distortion of the $\Omega(2012)^-$ peak in the lower tail region. By analyzing the asymmetric $\Omega(2012)^-$-peak structure, we may extract the mass and width of $\Omega(2002)^-$ even if the *LS* partner has the same mass as of $\Omega(2012)^-$ with a different width. The high statistic data would enable us to reveal the *LS* partner of $\Omega(2012)^-$. As for the Roper-like Ω^*, $\Omega(2160)^-$, having a broad width around 100 MeV, the corresponding events are distributed in a wide range, just forming a shoulder. A peak or bump would be clearly observed corresponding to each of the other Ω^*'s with narrower widths.

5. Summary

One of the fundamental goals of hadron physics is to understand hadron formation. Spectroscopic study of charmed and multi-strange baryons can provide unique information of internal structure of hadrons. Systematic spectroscopy experiment of charmed and multi-strange baryons are expected to reveal effective degrees of freedom and their interactions for the description of hadron structures. We consider the internal structure of the diquark with orbital excitation as an effective degrees of freedom. Different flavor combinations such as u, d, s quarks can lead to different properties. Therefore, a detailed knowledge of the spin dependent interaction for u, d, s quarks is an essential issue that can be studied at π20 and K10 beam lines in the J-PARC hadron experimental facility. At the π20 and K10 beam lines, we conduct spectroscopy of charmed baryons (Y_c^{*+}) as well as that of Ω baryon. Y_c^{*+}'s are produced in the two-body $\pi^- p \to D^{*-} Y_c^{*+}$ reaction, and they are identified from the $p(\pi^-, D^{*-})$ missing mass. Similarly, Ω^*'s, are produced in $K^- p \to \Omega^{*-} K^+ K^{*0}$, and they are identified from the $p(K^-, K^+ K^{*0})$ missing mass. We will carry out systematic studies of charmed and multi-strange baryons using intense hadron beams.

References

[1] S. Navas *et al.*, [Particle Data Group], Phys. Rev. D **110**, 030001 (2024).

[2] H. Noumi *et al.*, *J-PARC Proposal E50: Charmed Baryon Spectroscopy via the (π, D^{*-}) reaction* (2012).

[3] S. I. Shim, A. Hosaka, and H. C. Kim, Prog. Theor. Exp. Phys. **2020**, 053D0 (2020).

[4] K. Shirotori *et al.*, *J-PARC Proposal P85: Spectroscopy of Omega Baryons* (2021).

[5] K. H. Tanaka, M. Ieiri, H. Noumi, M. Minakawa, Y. Yamanoi, Y. Kato, H. Ishii, Y. Suzuki, and M. Takasaki, *Optical design of beam lines at the KEK PS new experimental hall*, Nucl. Instrum. Meth. A **363**, edited by K. Ura, T. Matsuo, M. Hibino, M. Komuro, M. Kurashige, S. Kurokawa, S. Okayama, H. Shimoyama, and K. Tsuno, 114-119 (1995).

[6] K. Aoki *et al.*, *Extension of the J-PARC Hadron Experimental Facility: Third White Paper* arXiv:2110.04462 [nucl-ex] (2021).

[7] T. Aramaki *et al.*, ELPH annual report, Tohoku University 2018, **44** (2019).

[8] T. Akaishi *et al.*, ELPH annual report, Tohoku University 2018, **58** (2019).

[9] N. Tomida *et al.*, *Beam Ring Imaging Cherenkov Detector for the J-PARC MARQ Experiments*, PoS J-PARC2024 in press.

[10] R. Honda *et al.*, *Continuous timing measurement using a data-streaming DAQ system'*, Prog. Theor. Exp. Phys. **2021** 123H01 (2021).

[11] K. Shirotori *et al.*, *Test experiment of the trigger-less streaming-readout data acquisition system at the J-PARC hadron facility*, PoS J-PARC2024 in press.

[12] S. H. Kim, A. Hosaka, H. C. Kim, H. Noumi, and K. Shirotori, Prog. Theor. Exp. Phys. **2014**, 103D01 (2014).

[13] D. J. Crennell, H. A. Gordon, K.-W. Lai, and J. M. Scarr, Phys. Rev. D **6**, 1220 (1972).

[14] Y. Nara, N. Otuka, A. Ohnishi, K. Niita, and S. Chiba, Phys. Rev. C **61**, 024901 (2000).